A New Method for Zone Development Observation for Updraft Rice Husk Gasification

Kasemsil Onthong and Jarruwat Charoensuk *

Experiments were carried out with a new method for assessing an updraft gasification reactor. An attached side door enabled the investigation of zone development by stopping air supply at specific times, when the thickness of biomass, char, and ash layers were measured. Development in zone thicknesses of biomass, char, and ash with time associated with temperature distribution provided information about the speed of flame propagation inside the reactor. Initially, pyrolysis and volatile combustion occurred, as evidenced by the high mass loss rate and high growth rate of the char layer. Shrinkage in the char layer took place later, and this phenomenon was governed by char glowing, which was relatively slow in mass loss rate. Finally, the fully developed char layer was obtained. The results from four different air mass fluxes under updraft configuration were presented, showing the differences in layer development. Temperature profiles at each time step revealed that the location of peak temperature coincided with the location of ash-char interface for every air mass flux. This effect was due to the high energy release during the oxidation of fixed carbon.

Keywords: Biomass; Gasification; Updraft; New method; Pyrolysis; Volatile combustion

*Contact information: Department of Mechanical Engineering, Faculty of Engineering, King Mongkut's Institute of Technology Ladkrabang, Bangkok 10520, Thailand; *Corresponding author: jarruwat.ch@kmitl.ac.th*

INTRODUCTION

Liquid petroleum gas (LPG) consumption in Thailand is divided into four sectors, which are household, transportation, industrial, and petrochemical. The household sector accounted for 33% of total LPG consumption and was the largest in 2018 (EPPO 2018). Almost all of the household consumption is related to cooking with a burner. Burners are small, having a typical output within the range of 2 to 3 kW. It is important to reduce fuel consumption as it helps to reduce cost of living, which is considered one of the four basic human needs.

Biomass is a low cost energy resource in Thailand. It has an average cost of 5.66 x 10^{-5} baht/joule, while LPG costs approximately 5.11 x 10^{-4} baht/joule. Despite its low cost, biomass combustion is more complex than combustion of gaseous fuel. It is difficult to operate and not practical for cooking applications because of poor responses and low precision in tuning to meet specific thermal demands. These problems inhibit the use of biomass cooking stove among unskilled users.

There have been several developments and innovations in burners for household cooking using biomass as fuel. Most research focuses on different conditions in the operation of a conventional top-lift updraft (TLUD) design, with a major parameter of thermal efficiency (Ballard-Tremeet and Jawurel 1996; Reed and Larson 1996; Bhattacharya *et al.* 2002; Belonio *et al.* 2011; Belonio and Castillo 2012; Tryner *et al.*

2014; Shuanghui *et al.* 2015; Suresh *et al.* 2016; Sutar *et al.* 2017; Rasoulkhani *et al.* 2018; Dinesha *et al.* 2019; Jain and Sheth 2019). The reported thermal efficiency is in the range of 22% to 37%. More detailed investigation has been proposed with a combined gasification and syngas burner system. Various parameters that affect the operating conditions, including thermal efficiency, temperature distribution in the reactor, syngas temperature and composition, calculated cold gas efficiency (CGE), and the fuel size and type should be studied. The reported CGE ranges from 31% to 80%.

Biomass gasification studies are crucial pre-requisites for cooking burner development. There have been several attempts to maximize the efficiency of the complex indirect gasification process, but simple configurations, for example, updraft or downdraft types, are appropriate for small heating applications (Reed and Das 1988; Sheth and Babu 2009; Gai and Dong 2012; Teixeira *et al.* 2012).

Recent research has examined gasification of biomass under updraft and downdraft conditions, with a focus on the burning rate or smoldering propagation speed with different airflow supply and syngas composition (Reed and Das 1988; Horttanainen *et al.* 2002; Ryu *et al.* 2005; Ryu *et al.* 2007; Sheth and Babu 2009; Madhiyanon *et al.* 2011; Gai and Dong 2012; Teixeira *et al.* 2012; Dion *et al.* 2013; Chao *et al.* 2014; Mahapatra and Dasappa 2014b; James *et al.* 2015; Ma *et al.* 2015; Kim *et al.* 2016; Rasoulkhani *et al.* 2018; Xuan-Huynh *et al.* 2018; Susastriawan and Saptoadi Purnomo 2019). A similar problem exists in solid fuel combustion over a traveling grate, which is widely adopted for industrial boilers, where the burning rate is related to the fuel thickness layer over the grate. Various physico-chemical processes interact with each other during the operation, and the system is dealing with uncertainty, *e.g.*, abrupt changes in thermal demand. Understanding combustion under updraft conditions will enable engineers to optimize the process for specific plant operations.

In various studies on gasification stoves and combined gasification and syngas burner systems, there has been little research on the transient response of the system. This characteristic is very important in the operation and reliability of the system. As automation equipment becomes affordable at the domestic level, there will be more economic feasibility for various applications. Automation could alleviate the operation difficulties of gasification stoves and make them more practical for non-technical operators. To successfully control the reactor, it is necessary to understand the smoldering characteristics of packed bed fuel during gasification, *e.g.*, flame propagation during start up or operation under load variation, *etc*. Eventually, the operation algorithm could be transferred to a logical statement in an automation system.

In this paper, experiments were conducted with a new assessment method that allows the investigator to observe zone development inside the reactor. This was achieved by stopping air supply at a specific period of time. The information of zone development and temperature distribution evolution will provide insight to smoldering propagation phenomena under updraft configuration.

EXPERIMENTAL

Materials

Rice husk was used as fuel in this work. Its properties and heating values are shown in Table 1 (Madhiyanon *et al*. 2011).

Table 1. Proximate and Ultimate Analyses of Rice Husk

Ultimate Analysis (%, as received)					Proximate Analysis (%, as received)				
C	H	O	N	S	Volatile	Fixed carbon	Moisture	Ash	HHV (MJ/kg)
38.0	4.55	32.4	0.69	0.60	55.6	20.1	10.3	14.0	15.0

Methods

Fixed bed reactor

All experiments were conducted using an updraft fixed-bed gasification facility, as illustrated in Fig. 1a. The reactor had a 90-mm internal diameter and total height of 500 mm. The upper end of the reactor was fitted with a 100-mm free board chamber, and the lower end had a 100-mm air manifold. The fuel grate is designed for supplying uniform updraft air flow through the packed fuel bed. The air hole distribution of the grate was verified that it was small enough to prevent the fuel particle or the ash to fall down through the grate. This reactor was equipped with a unique side door with high temperature gasket allowing visual inspection of the evolution from biomass to char and ash at the specific time elapsed after the ignition process, as shown in Fig. 1b. The reactor was well insulated with ceramic fiber to prevent major heat loss. Fuel was fed into the top of the reactor through the container. Air mass flux was supplied from the bottom by air compressor pump. The internal reactor temperature was measured by nine K-type thermocouples integrated with a Yogokawa MW-100 temperature recording system (Yokogawa Electric Corporation, Tokyo, Japan) along the vertical axis of the reactor. The height of the packed bed was measured by a metering rod, which could be inserted from the top of the reactor during gasification.

Experimental procedure

Initially, 200 g of rice husk was placed in the reactor, allowing it to be randomly packed with a 400-mm height above the fuel grate. The ignition process was performed by introducing the air mass flux, in corresponding to each experimental case, to the air manifold port underneath the reactor. The propane torch was inserted at the ignition port just above the fuel grate. The torch then fired into the fuel bed. The grate temperature (T1) was monitored until it reached 100 °C, which allowed the pyrolysis flame to propagate upward from the fuel grate. At this point, the temperature recording system was activated.

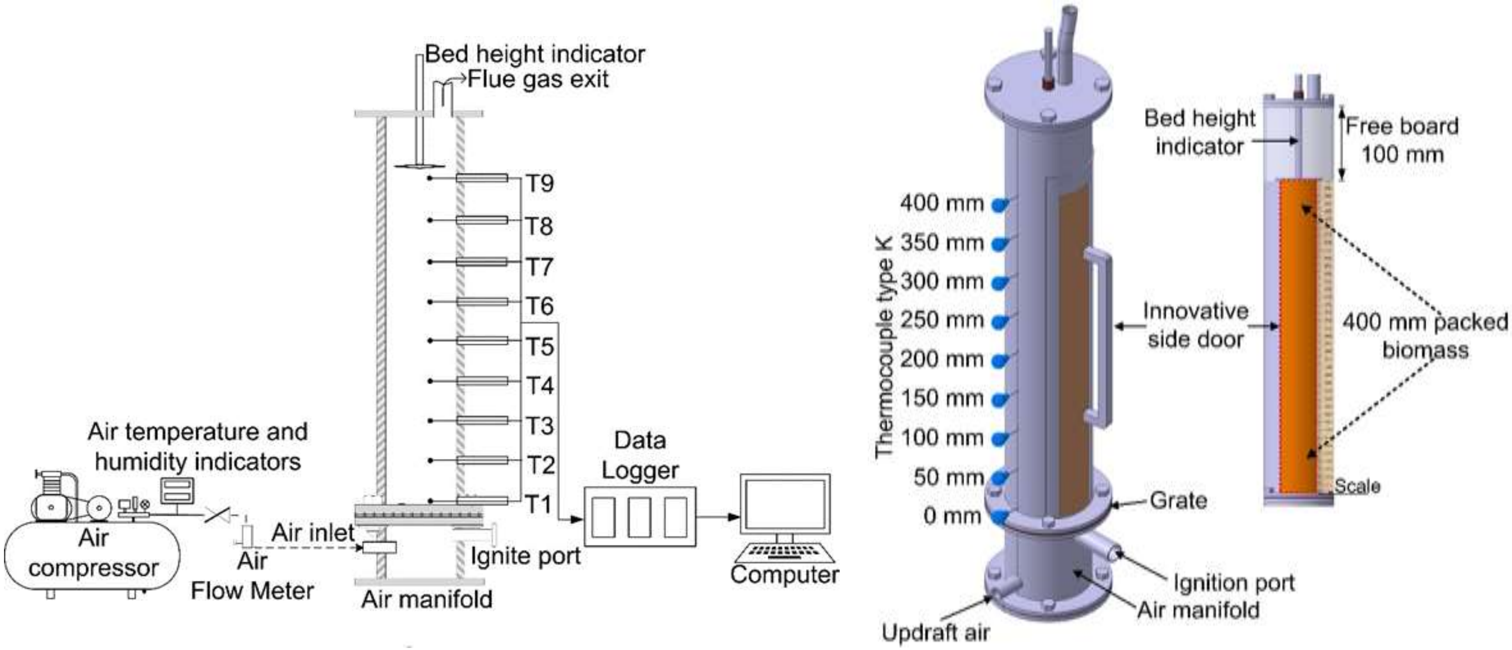

(a) (b)

Fig. 1. (a) Schematic diagram for updraft gasification; (b) configuration of the packed bed reactor used for updraft gasification

Calculation

Bed movement and the layer shrinkage and expansion were calculated as follows,

$$Ash_{shrinkage} = \frac{x_1 - x_2}{\Delta t} \quad (1)$$

$$Char_{shrinkage} = \frac{x_2 - x_3}{\Delta t} \quad (2)$$

$$Biomass_{shrinkage} = \frac{x_3 - x_4}{\Delta t} \quad (3)$$

$$Bed\ \ movement = \frac{x_5 - x_4}{\Delta t} \quad (4)$$

where $x_1 = 0$ is the reference grate location, x_2 is the distance between grate and ash and char interface layer, x_3 is the distance between grate and char and biomass interface layer, x_4 is the distance between grate and top of the biomass level, x_5 is the open top of the reactor, and Δt is the differential interval time period. Zone definitions are illustrated in Fig. 2.

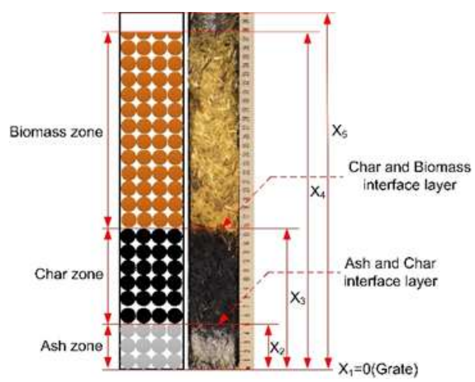

Fig. 2. Different zones in the reactor

The repeatability of this experiment was calculated as follows, (Kyu-Lee *et al.* 2015),

$$SE = \frac{SD}{\sqrt{n}} \quad (5)$$

where SE is the standard error, SD is the standard deviation, n is the number of samples.

The equivalent ratio (ER) was calculated using equation 6 (Basu 2010):

$$ER = \frac{Actual\ air}{Stoichiometric\ air}\ ,\ ER\ < \ 1\ (gasification) \quad (6)$$

Stoichiometric air was calculated in correspondence with the mass of rice husk loaded in the reactor (200g).

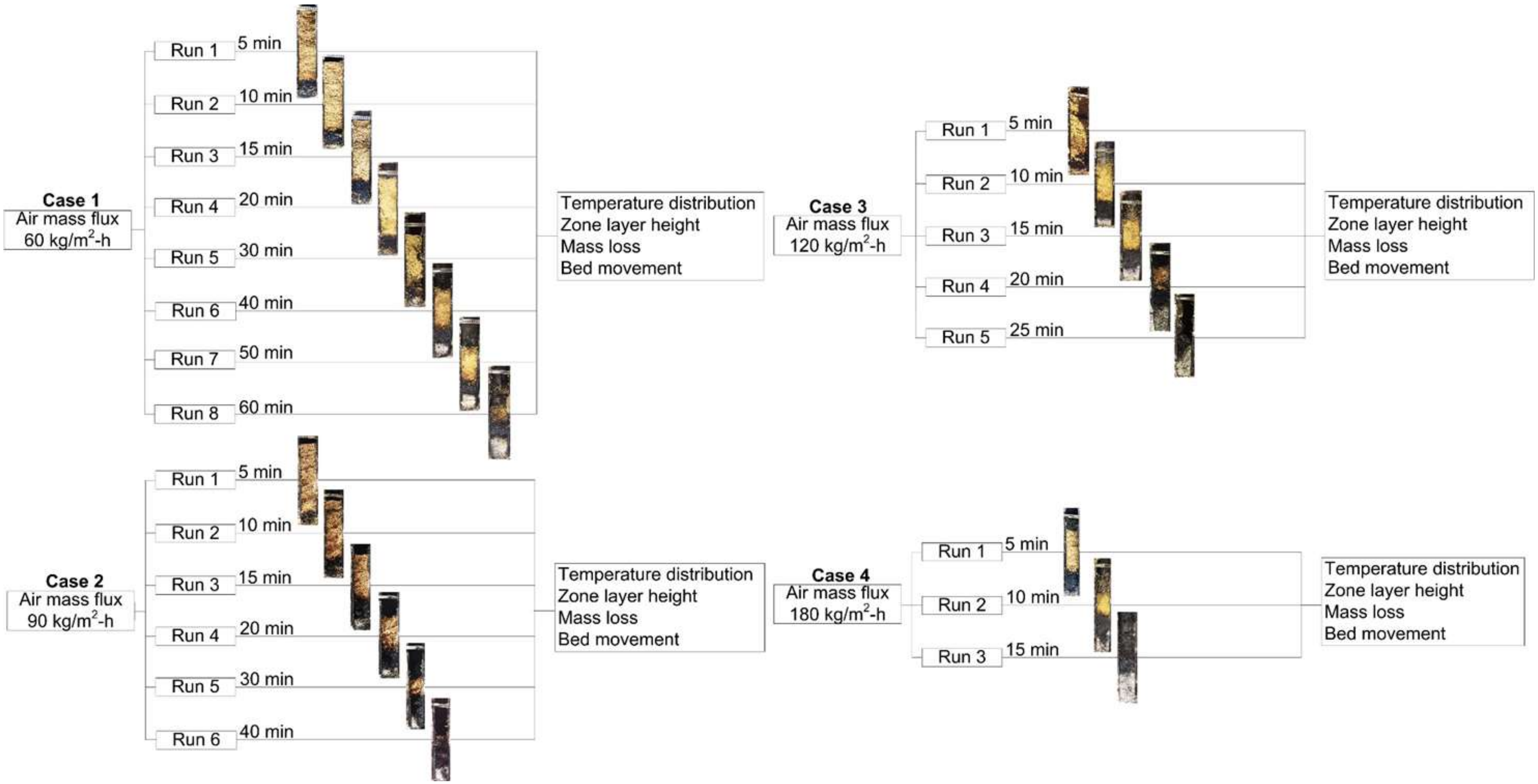

Fig. 3. Details of test trials

RESULTS AND DISCUSSION

Zone Development

Zone development and bed movement were observed by stopping air supply at specific periods of time. By doing so, the reaction was halted due to lack of oxidizer. The inlet air pipe and flue gas exit port were plugged to prevent any diffusion of air into the reactor. The reactor was allowed to cool to room temperature and opened for investigation. Thickness layers of biomass, char, and ash were measured for a specific time step. To obtain the development of these layers with time, the reactor was emptied and refilled with fresh fuel, and the entire operation procedure was repeated from the beginning and halted for the result of each time step. It was found that the maximum temperature was increased with the increasing equivalent ratio. This was in good agreement with other updraft gasification configuration (Rowland 2010; Manek *et al.* 2019). Visual observation was used to detect the ash, char, and biomass zones that developed in the reactor. Figure 3 shows details of test trials.

Air Mass Flux of 60 kg/m$^{2}\cdot$ h (ER = 0.50)

Figure 4 shows the zone development when applying the air mass flux at 60 kg/m^{2}h. The char zone was developed from the grate up to 75 mm in the first 5 min. The mass loss was also high (Fig. 16), while ash was not present. This result implied that homogeneous combustion of pyrolysis gas in pore cavities of the fuel bed was dominant in this period.

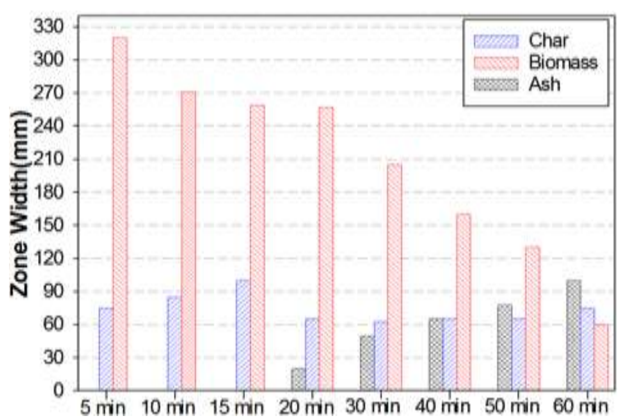

Fig. 4. Zone width at air mass flux 60 of kg/m^{2}hr

Pyrolysis and volatile combustion were coupled by thermal energy because combustion released heat from the bottom layer where fuel was ignited. Pyrolysis occurred nearby at layer above the ignition zone by absorbing the heat *via* convection and radiation. Finally, the combustion process was spread from the bottom layer until it reached the distance that the oxygen was depleted. This phenomenon was supported by the abrupt char growth layer of 75 mm within the initial period of 5 min. Massive evolution of smoke was observed at this period, which indicated condensation of steam and heavy hydrocarbon produced by pyrolysis into fine droplets on the top of the reactor when the gas was quenched to the atmospheric condition (Tar).

In the period between the time steps of the 5th and the 15th min from time of ignition, in accordance to Fig. 4, the pyrolysis rate was decreased, as observed by small changes in thickness of biomass layers that occurred between these two time steps, with the average rate around 4.06 mm/min. However, the bed temperature increased almost constantly at the rate between 18.46 °C/min. As suggested in Fig. 6, it could be postulated that char combustion was a dominant process during this second period. The mass loss rate was decreased, while the pyrolysis and homogeneous combustion mode switched to the char glowing mode. This observation coincided with a previous study (Ryu *et al*. 2007) and a single particle analysis of wood combustion (Mahapatra and Dasappa 2014a). Moreover, it was inferred that within the first 5 min from ignition, the pyrolysis zone grew more abruptly than the glowing rate of char combustion that occurred between the 5th and the 15th min from the initial state.

The temperature at the interphase between char and biomass layers at this period was 100 °C to 150 °C. This condition would have enabled the pyrolysis flaming to propagate if there had been residual oxygen in this region. Therefore, slow pyrolysis without combustion occurred at the char-biomass interphase together with char combustion layer at the grate that was related to a slow mass loss rate. Char glowing has a significantly lower burning rate than pyrolysis flaming (Ryu *et al*. 2007). Notably, there was very little smoke emitted from the top of the reactor, confirming that char glowing was a dominant process.

At the 20th min, the ash layer started to form at the fuel grate. The temperature of the grate (T_1) started to drop, and the combustible fuel at the grate started to burn out. The char layer shrank during the 20th to the 30th min because the bottom char layer had turned into ash, which is depicted in Figs. 4 and 5. Moreover, the weight loss rate of 10% (Fig. 16) was higher than the weight loss within the period of the 5th to the 15th min. As the char layer at the grate had burnt out leaving the incombustible ash behind, the combustion zone then shifted toward the upper location. The shrinkage in char layer led to an increase in heat transfer to the char-biomass interface, resulting in a higher rate of pyrolysis. Figure 4 shows an increase in biomass zone shrinkage from approximately 6.83 mm/min to 12.85 mm/min from the 20th min onward.

From the 20th to the 60th min, the zone development layers moved upward at an almost constant rate, indicating the pyrolysis and char burning rates were constant. Figure 4 indicates a decrease in biomass thickness layer at 4.92 mm/min. The char thickness layer was constant with the width around 65 to 75 mm, while the ash zone was growing at the rate of 2 mm/min. These changes made the rate of bed movement at 2.7 mm/min. Weight loss rate was measured at 1.95 g/min.

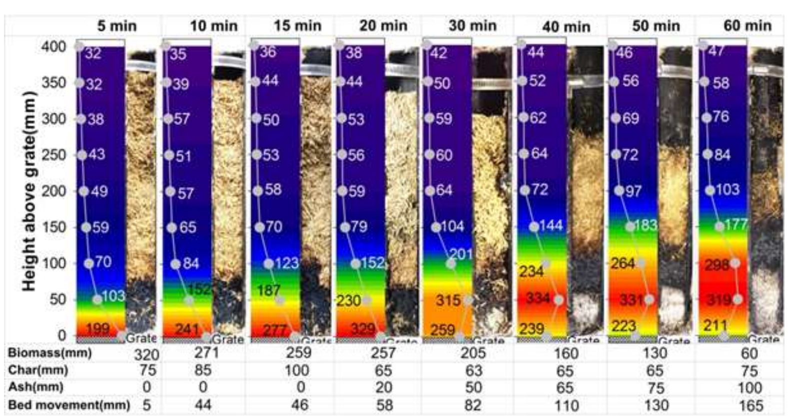

Fig. 5. Zone development at air mass flux of 60 kg/m^{2}h

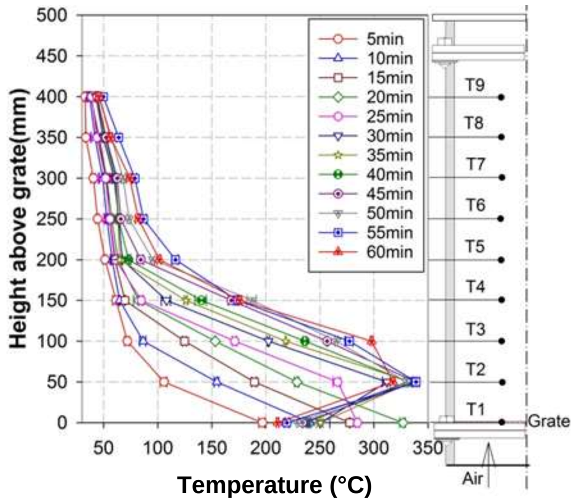

Fig. 6. Temperature distribution at different time in the reactor at air mass flux of 60 kg/m^{2}h

Air Mass Flux of 90 kg/m^{2}h (ER = 0.89)

During the first 5 min, the char growth rate was considerably less than the case with air mass flux of 60 kg/m^{2}h (Fig. 7), as it developed within 50 mm from the grate. The temperature above the grate was higher than in the earlier case (Figs. 8 and 9). Thus, the volatile combustion took place at a more intense rate than in the case of 60 kg/m^{2}h. Oxygen was consumed and depleted within less distance, resulting in a smaller heat-affected zone above the grate. A higher mass loss rate was observed (Fig. 16) during this period because of the dominant volatile combustion (Ryu *et al*. 2006). In contrast to the case of 60 kg/m^{2}h, a char layer shrinkage period was not observed for 90 kg/m^{2}h.

The ash layer started to form at the 15th min, as shown in Fig. 7, which was faster than the case of 60 kg/m^{2}h. The maximum grate temperature (maximum T_1) was 331 °C at the 20th min. The peak temperature was 433 °C (Fig. 8). This result coincided with the interface of the char and ash layer. In addition, it was evidence that the maximum grate temperature (T_1) at the 5th min was lower than the peak temperature, which occurred at the ash and char interface (above T_1) at the 10th min. This was due to higher energy release rate of char oxidation at the ash-char interface compared with the reaction of raw biomass at the grate of the reactor.

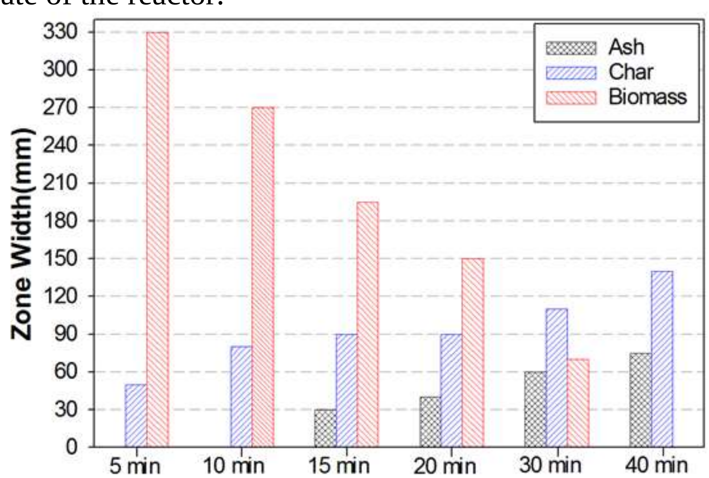

Fig. 7. Zone width at air mass flux of 90 kg/m^{2}h

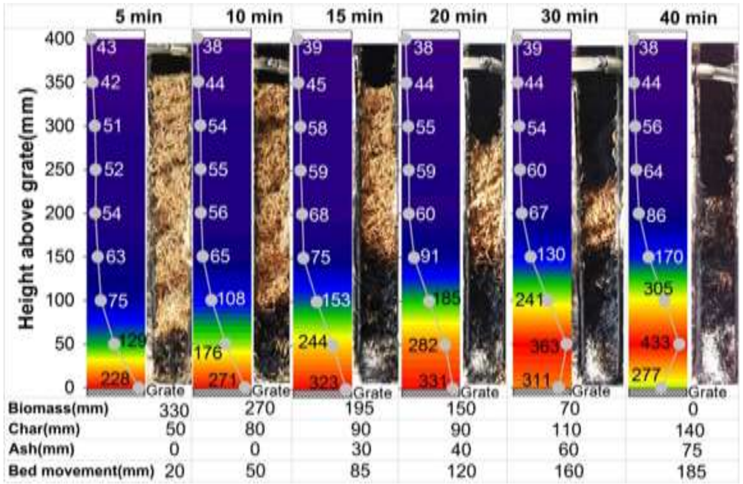

Fig. 8. Zone development at air mass flux of 90 kg/m^{2}h

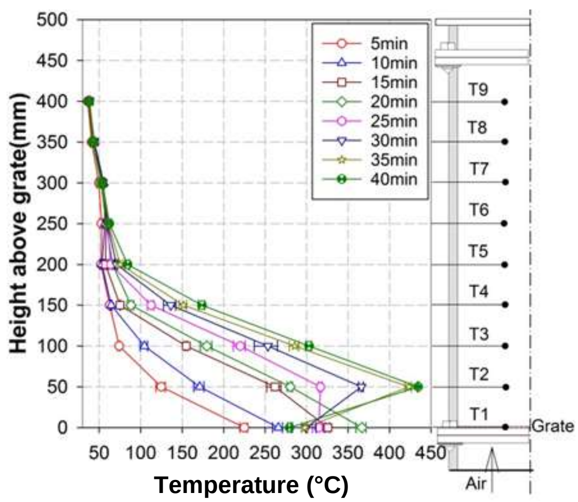

Fig. 9. Temperature distribution at different time in the reactor at air mass flux of 90 kg/m^{2}h

Air Mass Flux of 120 kg/m^{2}h (ER = 0.37)

The observed behavior was similar to the case with 90 kg/m^{2}hr air mass flux. Ash began to form during the first 5 min. The char growth rate was marginally higher than in the case with 90 kg/m^{2}h air mass flux. The char layer reached full development at the 10th min with the layer height of 100 mm. This was very similar to the result with 90 kg/m^{2}h. The char layer location had moved upward at the speed of 20 mm/min after the full development was reached. The maximum grate temperature (maximum T_1) was 437 °C, which was the same as the case with 90 kg/m^{2}h air mass flux, but occurred at the 10th min. The peak temperature was marginally higher than the case with 90 kg/m^{2}h air mass flux, which was 470 °C.

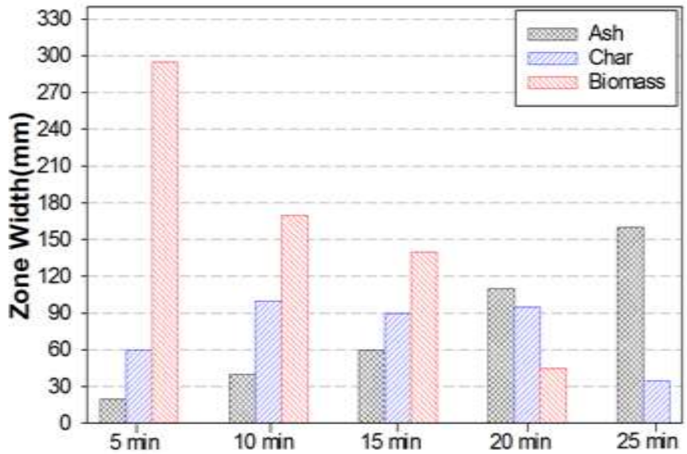

Fig. 10. Zone width at air mass flux of 120 kg/m^{2}h

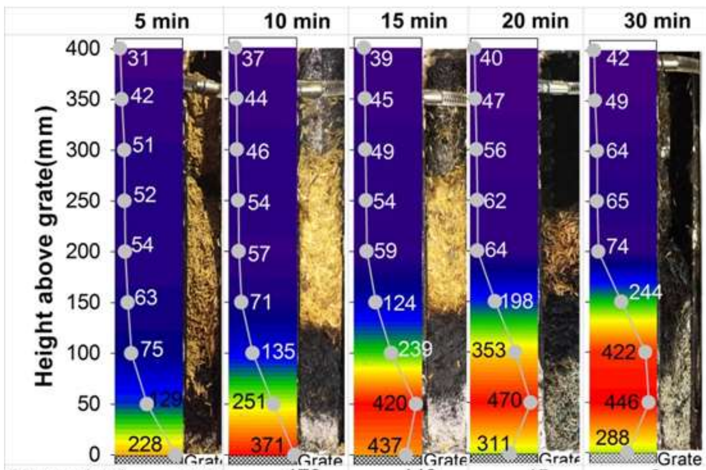

	5 min	10 min	15 min	20 min	30 min
Biomass(mm)	295	170	140	45	0
Char(mm)	60	100	90	95	35
Ash(mm)	20	40	60	110	160
Bed movement(mm)	25	90	110	150	205

Fig. 11. Zone development at air mass flux of 120 kg/m^{2}h

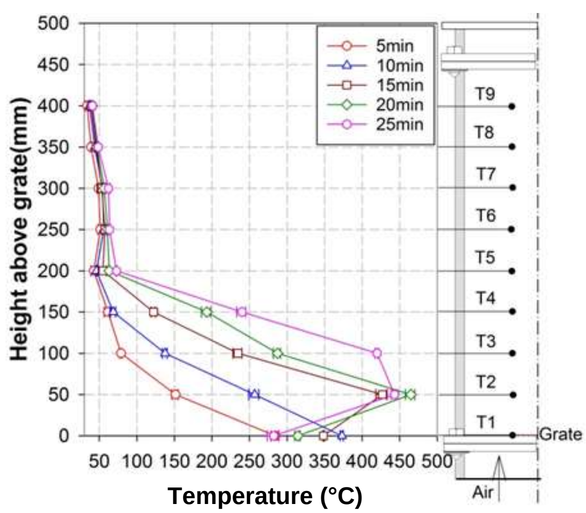

Fig. 12. Temperature distribution at different time in the reactor at air mass flux of 120 kg/m^{2}h

Air Mass Flux of 180 kg/m^{2}h (ER = 0.36)

More ash and char was formed during the first 5 min from ignition. Ash was formed with an average rate of 8 mm/min, which was considerably higher than the case of 120 kg/m^{2}h because of the average higher burning rate (Figs. 13 and 14). The maximum grate temperature (maximum T1) was around 348 °C, which was lower than in the case of 90 kg/m^{2}h and 120 kg/m^{2}h air mass flux. An increase in air supply rate resulted in a lower grate temperature in this range. It was suspected that stronger convection enhanced the heat loss rate from the volatile combustion zone above the grate.

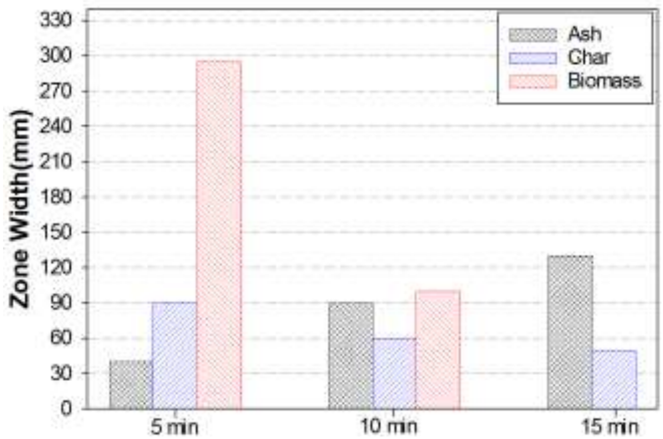

Fig. 13. Zone width at air mass flux of 180 kg/m^{2}hr

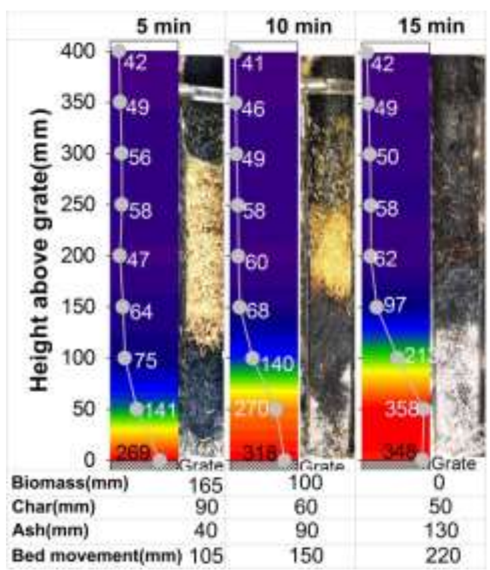

Fig. 14. Zone development at air mass flux of 180 kg/m^{2}h

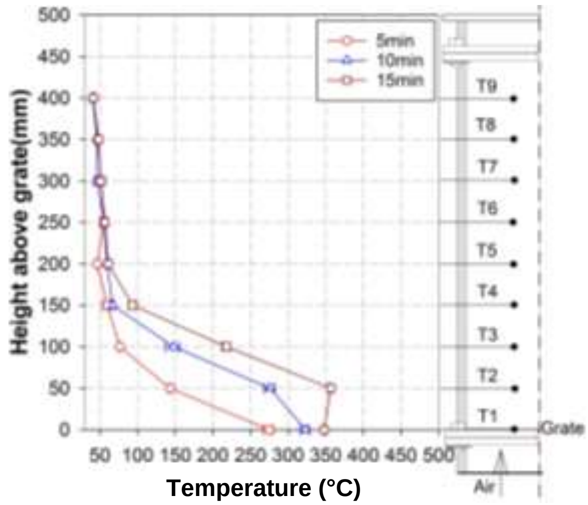

Fig. 15. Temperature distribution at different time in the reactor at air mass flux of 180 kg/m^{2}h

Temperature Profile

There are various endothermic and exothermic processes influencing the temperature profile in the reactor. During updraft gasification, it comprises a varying degree of drying, pyrolysis homogeneous combustion, and char glowing in the same location. This complexity is greatly reduced in one-dimensional problem analysis with reasonable assumptions and proper experimental setting up. In case of updraft gasification, the major heat transfer is convection in the flow direction and the radiation from temperature gradient along the bed.

The temperature profiles were similar for every tested case of input air mass flux. The constant negative gradient from the grate with peak temperature at the grate was observed. The temperature was increased with constant gradient after the ignition time. This result indicated that the volatile combustion and char glowing at the grate was intensified during this period. After that, an incombustible ash layer was formed at the grate, which was made apparent by the grate temperature drop (T_1). The peak temperature moved upward followed by the char and ash interface layer. The peak temperature at this interface was usually higher than the maximum temperature at the grate (maximum T_1).

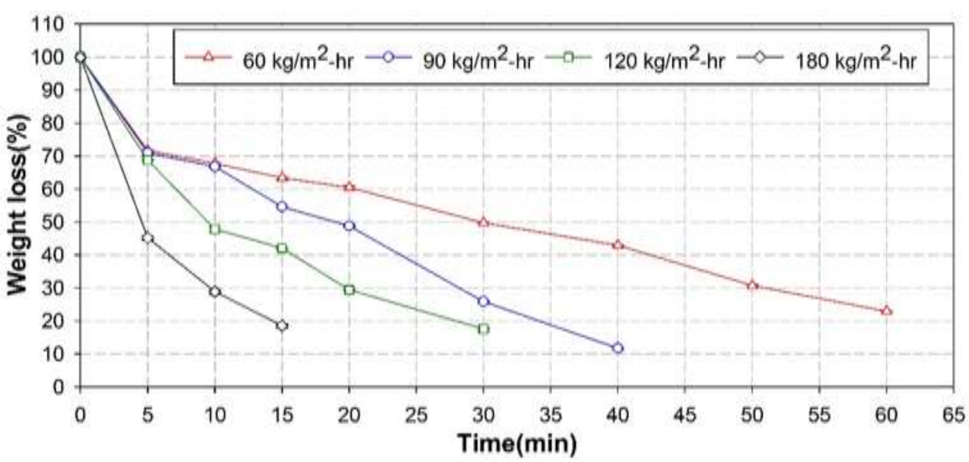

Fig. 16. Weight loss at air mass flux of 60, 90, 120, and 180 kg/m^{2}h

Bed Movement

There were two distinctive behaviors of bed movement, as shown in Fig. 17. First, high bed movement was observed during the first 15 min after ignition. This result implied pyrolysis and a volatile combustion period; the corresponding mass loss rate is revealed in Fig. 16. Secondly, the bed velocity appeared to reach steady velocity while the char layer was in a fully developed state.

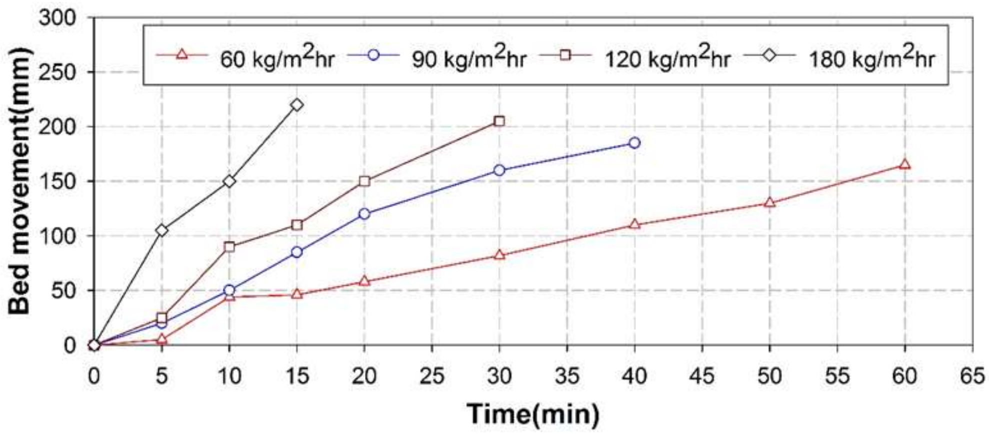

Fig. 17. Bed movement at air mass flux of 60, 90, 120, and 180 kg/m^{2}h

Standard Error

Standard error of the thermocouples number 1, 2, 3, and 4 was calculated for each specific time step and all experimental cases as shown in Fig 3. The reason for selecting only four thermocouples above grate was due to high temperature evolution at this region. The average standard error was not over 2.0 as can be seen in Fig. 18.

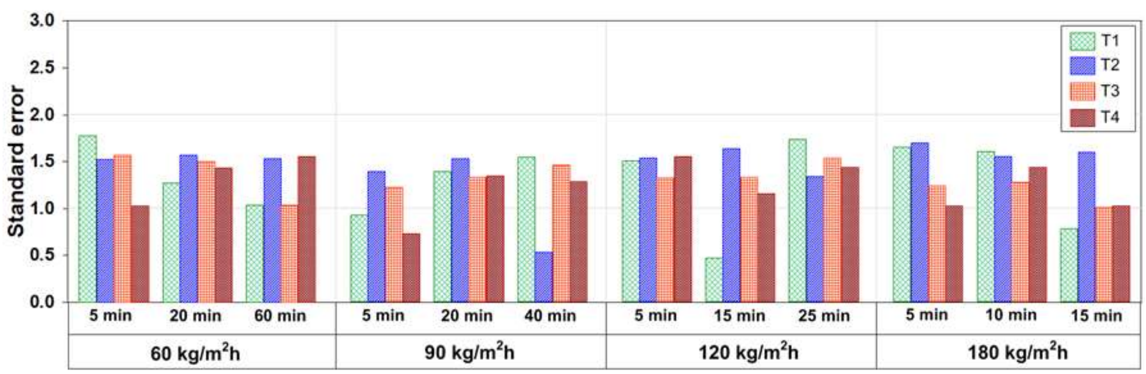

Fig. 18. Standard error of temperature

CONCLUSIONS

1. A new method for investigating the propagation under updraft conditions was developed using a reactor equipped with a side door, which enabled the investigator to explore zone development by stopping the air supply at specific periods of time. The zone development data gathered with temperature distribution evolution permitted better insights into smoldering propagation phenomena.
2. The layer development data revealed three distinctive periods in the propagation of rice husk fueled under updraft gasification, which were; i) pyrolysis and volatile combustion period, ii) char layer shrinkage, and iii) the fully developed period.
3. Peak temperature coincided with the ash and char interface layer positioning for every case of input air mass flux. Peak temperature was higher than the maximum grate temperature (maximum T_1). This was due to higher energy release rate of char oxidation at the ash-char interface as compared with the reaction of raw biomass at the grate of the reactor.
4. High mass loss rate was observed during pyrolysis and volatile combustion dominated period, which was the first period after the ignition for every input air mass flux.
5. Increasing the input air mass flux from 60 kg/m^{2}h to 90 kg/m^{2}h and 120 kg/m^{2}h resulted in overall increasing in temperature and the shrinkage of heat affected zone. However, further increases the input air mass flux to 180 kg/m^{2}h resulted in decreased maximum grate temperature (maximum T_1). It was suspected that stronger convection enhanced the heat loss rate from the volatile combustion zone above the grate.

REFERENCES CITED

Ballard-Tremeet, G., and Jawurek, H. H. (1996). “Comparison of five rural, wood-burning cooking devices: Efficiencies and emissions,” *Biomass and Bioenergy* 11(5), 419-430. DOI: 10.1016/S0961-9534(96)00040-2

Basu, P. (2010). *Biomass Gasification and Pyrolysis: Practical Design and Theory*, Academic Press, New York, NY.

Belonio, A., and Castillo, E. (2012). *Improved Versions of the Continuous-type Rice Husk Gas Stove for Household Use*, Technical Report of CRHET, Central Luzon State University Science City of Munoz, Nueva Ecija, Philippines.

Belonio, A., Sicat, E., and Cuaresma, F. (2011). *A Two-burner Continuous-type Rice Husk Gas Stove Developed for Household/Small Cottage Industry*, Technical Report of CRHET, Central Luzon State University Science City of Munoz, Nueva Ecija, Philippines.

Bhattacharya, S. C., Albina, D. O., and Khaing, A. M. (2002). “Effects of selected parameters on performance and emission of biomass fired cookstoves,” *Biomass and Bioenergy* 23, 387-395. DOI: 10.1016/S0961-9534(02)00062-4

Chao, C., Chunjiang, Y., Jinsong, Z., Yangyang, X., and Zhongyang, L. (2014). “Optimization of the three-stage biomass gasification characteristics in high-temperature entrained-flow bed,” *Bioresource Technology* 9(2), 2621-2633. DOI:

10.15376/biores.9.2.2621-2633

Dinesha, P., Kumar, S., and Rosen, M. A. (2019). "Performance and emission analysis of a domestic wick stove using biofuel feedstock derived from waste cooking oil and sesame oil," *Renewable Energy* 136, 342-351. DOI: 10.1016/j.renene.2018.12.118

Dion, L.-M., Lefsrud, M., Orsat, V., and Cimon, C. (2013). "Biomass gasification and syngas combustion for greenhouse CO_2 enrichment," *BioResources* 8(2), 1520-1538. DOI: 10.15376/biores.8.2.1520-1538

EPPO. (2018). *Report Energy Statistics of Thailand 2018*, Ministry of Energy, Thailand, Retrieved from http://www.eppo.go.th/images/Energy-Statistics/energyinformation/Energy_Statistics/00All.pdf

Gai, C., and Dong, Y. (2012). "Experimental study on non-woody biomass gasification in a downdraft gasifier," *International Journal of Hydrogen Energy* 37, 4935-4944. DOI: 10.1016/j.ijhydene.2011.12.031

Horttanainen, M., Saastamoinen, J., and Sarkomaa, P. (2002). "Operational limits of ignition front propagation against airflow in packed beds of different wood fuels," *Energy Fuels* 16, 676-686. DOI: 10.1021/ef010209d

Jain, T., and Sheth, P. N. (2019). "Design of energy utilization test for a biomass cook stove: Formulation of an optimum airflow recipe," *Energy* 166, 1097-1105. DOI: 10.1016/j.energy.2018.10.180

James, A. M., Yuan, W., Boyette, M. D., and Wang, D. (2015). "The effect of air flow rate and biomass type on the performance of an updraft biomass gasifier," *BioResources* 10(2), 3615-3624. DOI: 10.15376/biores.10.2.3615-3624

Kim, M., Lee, Y., Park, J., Ryu, C., and Ohm, T. I. (2016). "Partial oxidation of sewage sludge briquettes in a updraft fixed bed," *Waste Management* 49, 204-211. DOI: 10.1016/j.wasman.2016.01.040

Kyu-Lee, D., Junyong, I., and Sangseok Lee, S. (2015). "Standard deviation and standard error of the mean," *Korean Journal of Anesthesiology* 68(3), 220-223. DOI: 10.4097/kjae.2015.68.3.220

Ma, Z., Ye, J., Zhao, C., and Zhang, Q. (2015). "Gasification of rice husk in a downdraft gasifier: The effect of equivalence ratio on the gasification performance, properties, and utilization analysis of byproducts of char and tar," *BioResources* 10(2), 2888-2902. DOI: 10.15376/biores.10.2.2888-2902

Madhiyanon, T., Sathitruangsak, P., and Soponronnarit, S. (2011). "Effect of swirl secondary air injection on rice husk combustion in a short-combustion-chamber fluidized bed combustor using nozzle-type air distributor," *Journal of Research and Applications in Mechanical Engineering* 1, 77-82.

Mahapatra, S., and Dasappa, S. (2014a). "Experiments and analysis of propagation front under gasification regimes in a packed bed," *Fuel Processing Technology* 121 , 83-90. DOI: 10.1016/j.fuproc.2014.01.011

Mahapatra, S., and Dasappa, S. (2014b). "Influence of surface area to volume ratio of fuel particles on gasification process in a fixed bed," *Energy for Sustainable Development* 19, 122-129. DOI: 10.1016/j.esd.2013.12.013

Manek, B., Javia, M. S., Harichandan, A., and Ramani, H. (2019). "A CFD based comprehensive study of coal-fired updraft gasifier in ceramic industry," *Thermal Science and Engineering Progress 9*, 11–20. DOI: 10.1016/j.tsep.2018.11.001

Rasoulkhani, M., Ebrahimi-Nik, M., Abbaspour-Fard, M. H., and Rohani, A. (2018). "Comparative evaluation of the performance of an improved biomass cook stove and the traditional stoves of Iran," *Sustainable Environment Research* 28, 438-443. DOI:

10.1016/j.serj.2018.08.001
Reed, T. B., and Larson, R. (1996). "A wood-gas stove for developing countries," *Energy for Sustainable Development* 3(2), 34-37. DOI: 10.1016/S0973-0826(08)60589-X
Reed, T. B, and Das, A. (1988). *Handbook of Biomass Downdraft Gasifier Engine Systems*, Solar Energy Research Institute, National Renewable Energy Laboratory, Golden, CO, USA. DOI: 10.2172/5206099
Rowland, S. (2010). *Design and Testing of a Small-Scale Updraft Gasifier for Gasification of Eastern Redcedar*. M.Sc. Thesis, Oklahoma State University, Stillwater, OK, USA.
Ryu, C., Phan, A. N., Sharifi, V. N., and Swithenbank, J. (2007). "Co-combustion of textile residues with cardboard and waste wood in a packed bed," *Experimental Thermal and Fluid Science* 32, 450-458. DOI: 10.1016/j.expthermflusci.2007.05.008
Ryu, C., Yang, Y. B., Khor, A., Yates, E. N., Sharifi, V. N., and Swithenbank, J. (2006). "Effect of fuel properties in biomass combustion: Part I. Experiments-fuel type, equivalence ratio and particle size," *Fuel* 85, 1039-1046. DOI: 10.1016/j.fuel.2005.09.019
Sheth, P. N., and Babu, B. V. (2009). "Experimental studies on producer gas generation from wood waste in a downdraft biomass gasifier," *Bioresource Technology* 100, 3127-3133. DOI: 10.1016/j.biortech.2009.01.024
Shuanghui, D., Xuebin, W., Houzhang, T., Yan, L., Zhongfa, H., and Ben, N. (2015). "Optimization of operating conditions of a household up-draft biomass gasification stove," *BioResources* 10(3), 4178-4190. DOI: 10.15376/biores.10.3.4178-4190
Suresh, R., Singh, V.K., Malik, J. K., Datta, A., and Pal, R. C. (2016). "Evaluation of the performance of improved biomass cooking stoves with different solid biomass fuel types," *Biomass and Bioenergy* 95, 27-34. DOI: 10.1016/j.biombioe.2016.08.002
Susastriawan, A. A. P., and Saptoadi Purnomo, H. (2019). "Effect of tuyer distance above grate on propagation front and performance of downdraft gasifier with the feedstock of rice husk," *Renewable Energy* 134, 1034-1041. DOI: 10.1016/j.renene.2018.11.110
Sutar, K. B., Kohli, S., and Ravi, M. R. (2017). "Design and development and testing of small downdraft gasifiers for domestic cook stoves," *Energy* 124, 447-460. DOI: 10.1016/j.energy.2017.02.076
Teixeira, G., Steene Van De, L., Martin, E., Gelix, F., and Salvador, S. (2012). "Gasification of char from wood pellets and from wood chips: Textural properties and thermochemical conversion along a continuous fixed bed," *Fuel* 102, 514-524. DOI: 10.1016/j.fuel.2012.05.039
Tryner, J., Willson, B. D., and Marchese, A. J. (2014). "The effects of fuel type and stove design on emissions and efficiency of natural-draft semi-gasifier biomass cookstoves," *Energy for Sustainable Development* 23, 99-109. DOI: 10.1016/j.esd.2014.07.009
Xuan-Huynh, P., Piriou, B., Salvador, S., Valette, J., and Steene, L. (2018). "Oxidative pyrolysis of pine wood, wheat straw and miscanthus pellets in a fixed bed," *Fuel Processing Technology* 178, 226-235. DOI: 10.1016/j.fuproc.2018.05.029

Article submitted: January 28, 2019; Peer review completed: April 7, 2019; Revisions accepted: April 30, 2019; Published: May 7, 2019.
DOI: 10.15376/biores.14.3.5080-5096